Mdy2, a ubiquitin-like (UBL)-domain protein, is required for efficient mating in *Saccharomyces cerevisiae*

Zheng Hu, Bernd Potthoff, Cornelis P. Hollenberg and Massoud Ramezani-Rad*

Institut für Mikrobiologie, Heinrich-Heine-Universität Düsseldorf,Universitätsstrasse 1, Geb. 26.12, 40225 Düsseldorf, Germany
*Author for correspondence (e-mail: ramezani@uni-duesseldorf.de)

Summary

MDY2, a gene required for efficient mating of the yeast *Saccharomyces cerevisiae*, was characterized in this study. The gene encodes a protein of 212 amino acids, which contains a ubiquitin-like (UBL) domain (residues 74-149). Deletion of *MDY2* is associated with a five- to sevenfold reduction in mating efficiency, mainly due to defects in nuclear migration and karyogamy at the prezygotic stage. However, prior to mating pair fusion, shmoo formation is reduced by 30%, with a concomitant failure to form mating pairs. Strikingly, migration of the nucleus into the shmoo tip is also delayed or fails to occur. In addition, we show that in *mdy2* mutants, microtubule bundles, as well as the microtubule end-binding protein Kar9, fail to localize properly to the shmoo tip, suggesting that the nuclear migration defect could be due to aberrant localization of Kar9. Pheromone signal transduction (as measured by *FUS1* induction by α-factor) is not affected in *mdy2Δ* mutants and mitosis is also normal in these cells. *MDY2* is not induced by mating pheromone. In vegetatively growing cells, GFP-Mdy2 is localized in the nucleus, and remains nuclear after exposure of cells to α-factor. His-tagged Mdy2 shows no evidence of the C-terminal processing typical of ubiquitin, and also localizes to the nucleus. Thus *MDY2* is a novel gene, whose product plays a role in shmoo formation and in nuclear migration in the pre-zygote, possibly by interacting with other UBL-type proteins that possess ubiquitin association (UBA) domains.

Supplementary material available online at
http://jcs.biologists.org/cgi/content/full/119/2/322/DC1

Key words: Mating, Nuclear migration, Shmoo formation, Ubiquitin-like protein, Yeast

Introduction

Haploid *S. cerevisiae* cells occur in two mating types, **a** and α, and mating begins when cells of opposite mating type recognize each other by means of pheromones. *MAT*α cells secrete α-factor, whereas *MAT***a** cells secrete a-factor. The receptors for a-factor and α-factor are encoded by *STE3* in *MAT*α cells and *STE2* in *MAT***a** cells respectively, and belong to the large family of G-protein-coupled receptors that have seven transmembrane domains (Burkholder and Hartwell, 1985; Sprague et al., 1983). The binding of pheromone to receptor stimulates three major responses: (1) transcriptional induction of genes involved in mating, (2) arrest of the cells in G_1 phase, and (3) changes in cell morphology (for a review, see Herskowitz, 1995). The targets affected include genes whose functions are required for pheromone production and the pheromone response, and genes for proteins that facilitate or actually participate in cell pairing, cell cycle arrest and subsequent recovery from the arrested state, and mediate the morphological changes required for mating (Sprague and Thorner, 1992). One of the earliest effects of pheromone binding is cell cycle arrest late in the G_1 phase, prior to bud emergence, spindle pole body (SPB) duplication and DNA synthesis. Morphological changes ensue because mating cells sense the direction of the source of pheromone emanating from a mating partner (Segall, 1993). The receiving cell then undergoes polarized growth, forming a projection that is directed towards the signal source. This chemotropic response is thought to involve the generation of an internal landmark that reflects the direction of incidence of the external pheromone signal and overrides the spatial cues that normally control bud formation (Arkowitz, 1999; Chant, 1999).

Formation of the mating projection is mediated by the actin cytoskeleton and requires many other proteins (e.g. Spa2, Pea2, Bem1 and Cdc42) that are otherwise involved in bud emergence (Chenevert et al., 1994; Johnson and Pringle, 1990; Leeuw et al., 1995; Sheu et al., 1998). Components of the cytoskeleton, secretory system, plasma membrane and cell wall become asymmetrically reorganized along the axis defined by the pheromone source (Herskowitz et al., 1995; Matheos et al., 2004; Nern and Arkowitz, 2000; Read et al., 1992; Roemer et al., 1996), and the mating projection serves to concentrate the proteins involved in signalling (pheromones and pheromone receptors), cell adhesion (agglutinins) and fusion (Fus2) in the area of future cell contact and fusion. Thus, the proteins (α-factor, a-factor, Ste2, Ste3) that function specifically in these processes are all highly localized to the mating projections or their tips (Elion, 1995; Sprague and Thorner, 1992; Trueheart and Fink, 1989). Polarized mating cells, which are referred to as 'shmoos', signal to one another through their projections, and thereby mutually restrict growth to the sites of cell contact and fusion. Many polarization-related genes also function in the cell fusion pathway, as indicated by the cell fusion defects

observed in strains that are mutant for such genes (e.g. *SPA2*, *PEA2*, *BNI1*, *RVS161*, *PRM1*) (Dorer et al., 1997; Heiman and Walter, 2000).

Cell fusion usually occurs at the tips of the projections by formation of a conjugation tube or bridge. Nuclear fusion (karyogamy) is the last stage in the mating process and involves at least two steps. First, cytoplasmic microtubules emanating from the SPB bring the nuclei into close proximity, in a process called congression. The second step, karyogamy, entails the fusion of the nuclear membranes (for review, see Rose, 1996). The zygote then undergoes meiosis, and subsequently re-enters the vegetative cell cycle.

Although the cytological events involved in yeast mating have been well described, the molecular components and mechanisms important for mating cell morphogenesis, cell fusion and nuclear fusion are not well understood.

In the context of the EUROFAN project, deletion of *YOL111c* was shown to cause defects in mating (Iwanejko et al., 1999) (our unpublished data). In a subsequent study, Saeki et al. (Saeki et al., 2002) investigated whether Yol111c could bind to 20S proteasomes or ubiquitin chains, but could not find evidence for either. Here we present the results of an analysis of *YOL111c*, which we have renamed *MDY2* (for mating-deficient yeast). *MDY2* encodes a 212-residue protein, which contains an ubiquitin-like (UBL) domain. Its closest homologue is the 157-amino acid protein GdX found in humans. Here we present a phenotypic analysis of *mdy2* mutants and conclude that Mdy2 directly or indirectly plays a role in shmoo formation and nuclear migration in the pre-zygote.

Results

Deletion of *MDY2* results in a reduction in mating efficiency

The *MDY2* gene was identified in the course of the EUROFAN project on the basis of the mating defect observed in a mutant in which the ORF *yol111c* was disrupted in strain S288c. The first step in the characterization of *MDY2* was the complete deletion of the gene using the *LoxP-KanMX-LoxP* gene disruption cassette (Gueldener et al., 1996) in the W303 strain background, and the subsequent analysis of mating efficiency using a quantitative mating assay (see Materials and Methods). As shown in Fig. 1A, the efficiency of diploid formation in the cross *MAT**a** mdy2* × *MAT*α *MDY2* was 4±0.4% and in the reciprocal cross 6±1.3%; the corresponding value for the bilateral mutant cross was 3±0.9%. The wild-type strain shows a mating efficiency of 19±2.9%. Thus deletion of the *MDY2* gene results in a five to sevenfold reduction in mating efficiency. Taken together, mating against a wild-type strain gave a higher mating efficiency (four- to fivefold) than mating involving two mdy2 mutants (five- to sevenfold). The effect of *MDY2* deletion on the mating efficiency of *MAT**a*** cells was slightly stronger than that on *MAT*α cells.

Analysis of the shmoo index in crosses involving *mdy2* deletion mutants

Mating pheromones block the *S. cerevisiae* cell cycle in G_1 at START, and thus allow the cells to enter the mating pathway. G_1-arrested mating cells become large and pear-shaped (forming shmoos) as a result of mating projection formation, which allows them to aggregate, fuse and undergo karyogamy

(Andrews and Herskowitz, 1990; Cross et al., 1988). To identify the step affected by deletion of *MDY2*, we first examined G_1 arrest and shmoo formation in the *mdy2* mutant. Fig. 1B shows that the rate of α-factor-induced shmoo formation in *MAT**a** mdy2* cells was reduced compared to wild-type cells. The incidence of G_1 arrest was decreased only slightly (data not shown). In the wild-type strain a maximum of 73% of the cells have been transformed into shmoos after 2 hours of exposure to α-factor, whereas only about 47% of *mdy2*
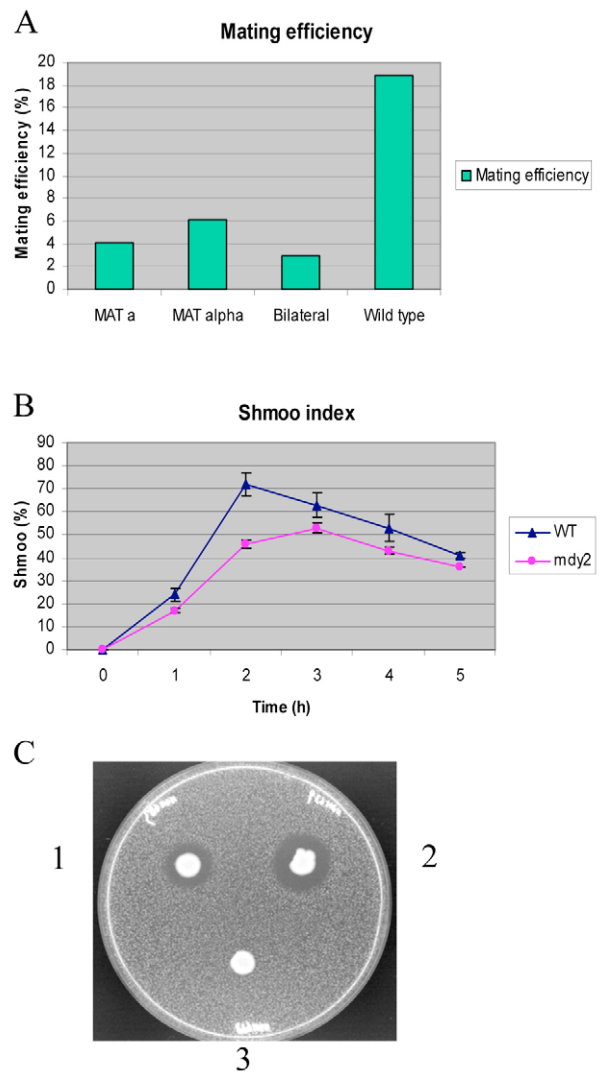

Fig. 1. Deletion of *MDY2* results in a reduction in mating efficiency. (A) Quantitative assay for the mating performance of different *mdy2* deletants. Values are means of two independent experiments, and represent the percentage of diploids in the cultures. (B) Shmoo index. Cultures of *mdy2* mutant (HZH686) and wild-type (W303-1A) strains were grown to log phase and treated with α-factor (final concentration: 5 μM). Aliquots were taken after different times of incubation and the numbers of shmoos in samples of at least 300 cells were counted. (C) Halo assay for α-factor production. 0.6% top agar was mixed with 10^5 indicator cells (*MAT**a** sst1*). Aliquots (approximately $4×10^6$ cells) of wild-type W303-1B (*MAT*α) and W303-1A (*MAT**a***) wild-type and *mdy2* mutant cells were spotted directly onto the top agar. The plate was incubated at 30°C for 2 days and photographed. 1. *MAT*α *mdy2* mutant cells (HZH683). 2. *MAT*α wild-type cells (W303-1B). 3. *MAT**a*** wild-type cells (W303-1A).

mutant cells were converted into shmoos by such treatment. The rest of the cells showed no projections. The mutant thus shows an approximate 30% reduction in shmoo formation in comparison to the wild-type strain. The ability to recover from pheromone exposure is also impaired in the mutant. The fact that G1 arrest is not significantly altered indicates that the signal transduction pathway activated by pheromone reception is functional in *mdy2* cells.

Next, production of a-factor and α-factor was assessed by assaying for growth inhibition of pheromone-supersensitive strains in plate halo assays. Fig. 1C shows that the halo formed by the *MAT*α *mdy2* mutant was smaller than that induced by the wild-type strain after 48 hours of incubation at 30°C (wild-type *MAT***a** was used as control). This observation is consistent with the results obtained with an *mdy2* deletion in the S288C background (results not shown) and suggests that the *MAT*α *mdy2* mutant is partially defective in the production or secretion of α-factor. The difference in halo size induced by *MAT*α cells was not a consequence of reduced growth rate since the mutants did not show a significant growth defect with respect to the wild-type isogenic strains (data not shown). We then investigated whether the defect in α-factor production can be compensated for by mating to a supersensitive strain (*sst2* or *bar1*). *mdy2* crosses with *MAT*α *sst2* (HGX133) or *MAT***a** *bar1* (HZH350) showed a three- to fourfold reduction in mating efficiency relative to crosses of wild-type strains with *MAT*α *sst2* or *MAT***a** *bar1*, compared to the four- to fivefold reduction seen with non-supersensitive strains. Production of a-factor appeared to be normal when tested on a lawn of sensitized *MAT*α *sst2* cells (supplementary material Fig. S1). Taken together, these findings demonstrate that changes in pheromone levels cannot account for the *mdy2* mating phenotype.

Formation of mating pairs and zygotes is impaired in crosses involving *mdy2* cells

In the quantitative mating assay *mdy2* mutants showed a five to sevenfold reduction in mating efficiency relative to wild type. Since the effects of the *mdy2* mutation on the pheromone response pathway were relatively weak, the subsequent steps in the mating process were studied.

We first determined the number of mating pairs (pre-zygotes and zygotes) formed in mating mixtures of *mdy2* and wild-type cells. After 2-4 hours of mating, *mdy2* cells had formed 30-40% fewer mating pairs than the wild-type control (Fig. 2A). The difference in the numbers of mating pairs was even more marked (60%) after 5 hours. This could be largely explained as a direct consequence of a failure to form shmoos.

In wild-type mating mixtures, zygotes accounted for 10, 18, 16 and 10% of total cells after 2, 3, 4 and 5 hours of incubation, respectively, whereas only 3, 6, 5 and 3% of *mdy2* mutants were zygotes at those time points (Fig. 2B).

To look specifically at the cell fusion phenotype in cells that formed shmoos, we performed a microscopic analysis of zygotes. Cell fusion was normal in *mdy2* zygotes, as judged by the quantitative analysis of cell fusion (Gammie and Rose, 2002) based on monitoring the redistribution of cytosolic GFP present in the *MAT***a** or MATα partner following the formation of mating pairs, and the appearance of a septum in unbudded zygotes (supplementary material Figs S4 and S5). The first mitotic division of the zygotic nucleus is not impaired in *mdy2* mutants.

To address the possibility that the deletion of *MDY2* results in an accumulation of pre-zygotic stages (zygotes that have not undergone karyogamy), we classified mating pairs into three groups: pre-nuclear fusion zygotes, normal zygotes and abnormal zygotes. More than 200 mating pairs formed by mixtures of *mdy2* and wild-type cells after a 3.5-hour incubation were analysed. In wild-type mating mixtures, pre-nuclear fusion zygotes accounted for nearly 17% of mating pairs, whereas 48% of *mdy2* mutant mating pairs were found to be of this type (Fig. 2C). In wild-type mating mixtures 74% of mating pairs were zygotes at this point, in contrast to 43% for *mdy2*. Moreover, the positions of the nuclei in *mdy2* pre-zygotes differ from those in the wild-type strain. In wild-type pairs the nuclei were closely juxtaposed, but in the *mdy2* zygotes they remained further apart (Fig. 3A). The difference was quantified by measuring the distance between the two haploid nuclei: in wild-type zygotes the approximate mean value was 3.6 μm and in *mdy2* zygotes 5.2 μm. This difference indicates that *mdy2* cells that have fused successfully are impaired in zygote formation (Fig. 3B).

To determine the subsequent fate of the nuclei in *mdy2* zygotes, the mating mixtures were analysed after 5.5 hours on YPD plates (Fig. 4). The zygotes were grouped into one of three classes according to the disposition of their nuclei: pre-nuclear fusion zygotes (class I, top row Fig. 4), post-nuclear fusion zygotes (class II, centre row), or zygotes in which mitotic division of haploid nuclei had occurred, indicating complete failure of karyogamy (class III, bottom row). As expected, after 5.5 hours most wild-type zygotes had completed nuclear fusion successfully and were in class II. By contrast, *mdy2* exhibited a higher percentage of pre-nuclear fusion zygotes (class I). Moreover, many more *mdy2* zygotes were in class III; i.e. karyogamy does not take place at all and the haploid nuclei undergo mitotic division (Fig. 4). Clearly, the *mdy2* defect leads to a marked delay in karyogamy, as demonstrated by the fact that 44% of the mutant zygotes belong to Classes I and III compared to only 12% of wild-type zygotes.

Cytoductants are haploid cells containing one parental nucleus in a mixed cytoplasm contributed by both parents. In wild-type matings the number of cytoductants produced is very low. However, in Kar⁻ zygotes, the presence of two unfused nuclei greatly increases the frequency of cytoductant buds. In order to test whether this occurs in matings involving *mdy2* cells, cytoductant analysis (Gammie and Rose, 2002) was performed (Table 1). As expected, *mdy2* × wild-type crosses showed a significantly higher cytoductant:diploid ratio (0.13 for *MAT***a** and 0.11 for *MAT*α) than wild-type × wild-type crosses (0.0053 for *MAT***a** and 0.0065 for *MAT*α).

The *mdy2* mutant shmoos exhibit a defect in nuclear migration

We next examined whether nuclear migration into pheromone-induced shmoos is defective in the *mdy2* mutant. *mdy2* and wild-type **a** cells were arrested by treatment with α-factor and scored for nuclear position using DAPI staining. In wild-type shmoos, the nucleus normally moves to the neck of the pear-shaped shmoo in preparation for mating (Miller and Rose, 1998; Read et al., 1992; Rose, 1991). In agreement with this observation, we found that in 40% of wild-type shmoos with projections (*n*=409) the nuclei were at the neck of, or in, the shmoo and in 4% of cells the nuclei were still on the opposite

side of the cell from the shmoo (Fig. 5A). By contrast, in only 20% of *mdy2* shmoos were the nuclei found in or at the shmoo neck, while 14% were on the side opposite the shmoo. Similar results were observed in strain S288c (data not shown). Since the nuclear envelope may be at some distance from the chromatin, we also determined the position of the nuclear envelope using a GFP-Nup116 fusion (Fig. 5B): Nup116 localizes to the nuclear pores (Fabre and Hurt, 1997). In 75%

of wild-type shmoos (*n*>300) GFP-Nup116 was at the neck of, or in, the projection; in 3% of cells the GFP-Nup116 signal was on the opposite side of the cell from the shmoo. By contrast, only in 40% of *mdy2* shmoos was the GFP-Nup116 found at the neck or in the shmoo, whereas 9% were on the side opposite the shmoo (Fig. 5B). These results are consistent with those obtained using DAPI staining, and confirm the presence of a defect in nuclear migration.
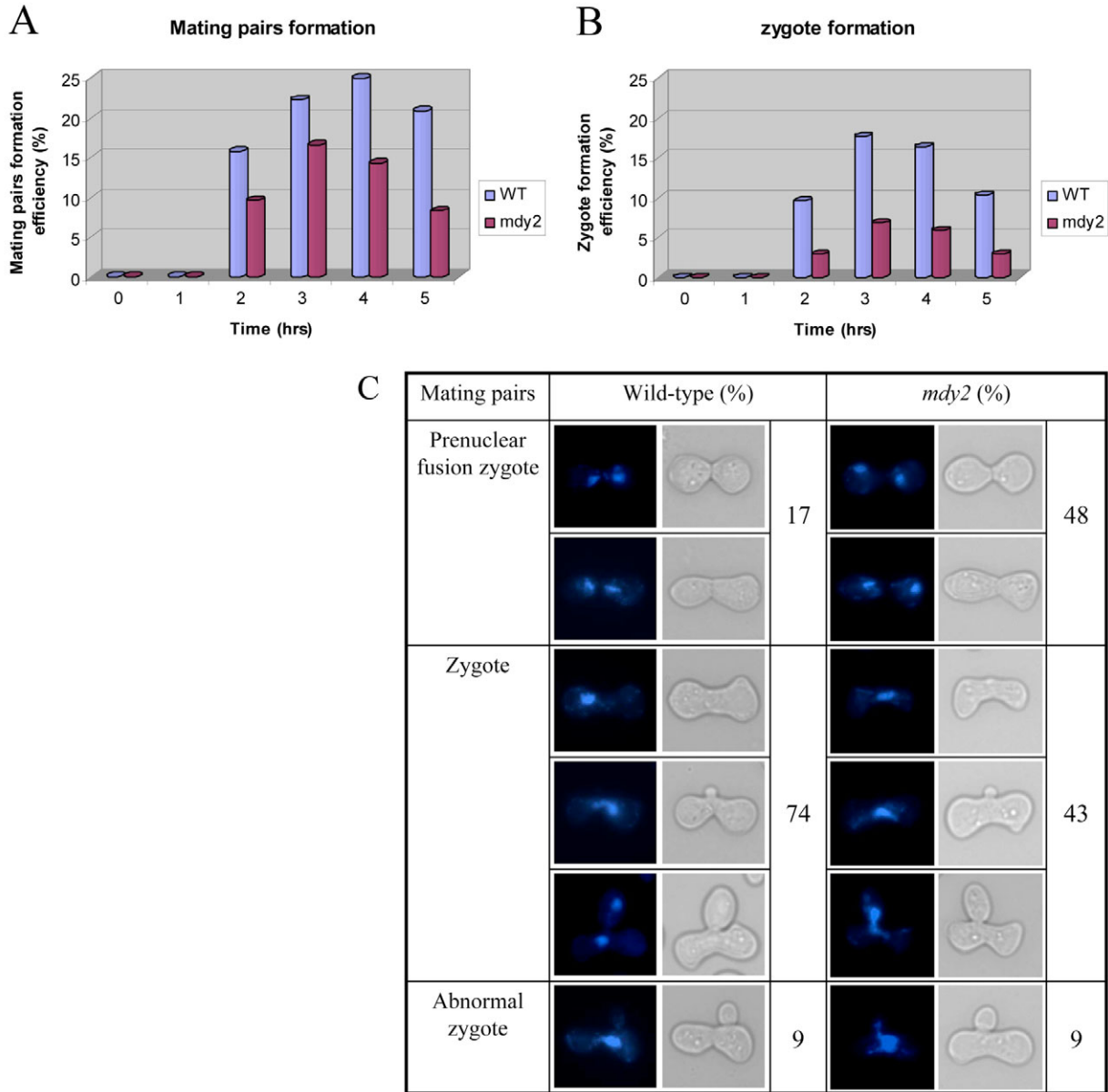
Fig. 2. Assay for zygote formation. (A) Mating pair formation. Cultures of opposite mating type of *mdy2* mutant (*MAT***a** and *MAT*α) and wild-type strains were grown to log phase. Equal numbers of cells (3×10^6) of each mating type were mixed with each other. The cell pellets were then transferred onto a NC membrane on an YPD plate and incubated at 30°C. Samples were taken after various times and the numbers of mating pairs in samples of at least 800 cells were counted. The percentage of mating pairs at each time point is shown. (B) Zygote formation. The same samples were used as in A and the nuclei were stained with DAPI, and the numbers of zygotes was counted. The percentage zygote formation is shown. (C) Classification of mating pairs. Cultures of *mdy2* mutant (*MAT***a** and *MAT*α) and wild-type strains of opposite mating type were grown to log phase. Equal numbers (3×10^6 cells) of each mating type were mixed, pelleted, transferred onto a NC membrane on an YPD plate and incubated at 30°C. Samples were taken after 3.5 hours incubation and stained with DAPI to identify zygotes and follow the course of karyogamy. The percentage of cells in the different stages of zygote formation was determined in samples containing at least 200 zygotes.

Thus the lack of Mdy2 seems to have two consequences. First, α-factor-induced shmoo formation is impaired, and second, migration of the nucleus is delayed or fails to occur. Since shmoo formation itself does not seem to be dependent on nuclear migration or attachment (Maddox et al., 2003), this might indicate the involvement of Mdy2 in an earlier function that affects both processes.

mdy2 mutants do not localize Tub1 and Kar9 to the shmoo tip properly

During mating, cytoplasmic microtubules are seen to enter the mating projection and apparently make contact with cortical sites (Carminati and Stearns, 1997; Miller and Rose, 1998). Thus, it seems likely that interactions between cortical proteins (like Kar9) and the cytoplasmic microtubules are a key element in nuclear migration and orientation. The cortical localization of Kar9 is particularly notable because it frequently intersects the ends of astral microtubules (Matheos et al., 2004; Miller and Rose, 1998). Since *mdy2* mutants exhibit defects in nuclear migration, we wanted to examine microtubule patterns (using GFP-Tub1) and Kar9 localization (using GFP-Kar9) (Fig. 6). In the wild-type shmoos, 77% of cells had a single bundle of cytoplasmic microtubules extending into the shmoo tip; 9% contained a single bundle of cytoplasmic microtubules directed toward the shmoo tip and a second bundle pointing away from the shmoo tip; 14% exhibited misoriented microtubules that were not near the shmoo tip. By contrast, only 35% of the *mdy2* cells had a single bundle of cytoplasmic microtubules going to the shmoo tip and 29% contained a single bundle of cytoplasmic microtubules going to the shmoo tip plus an additional bundle directed away from the shmoo tip. There was
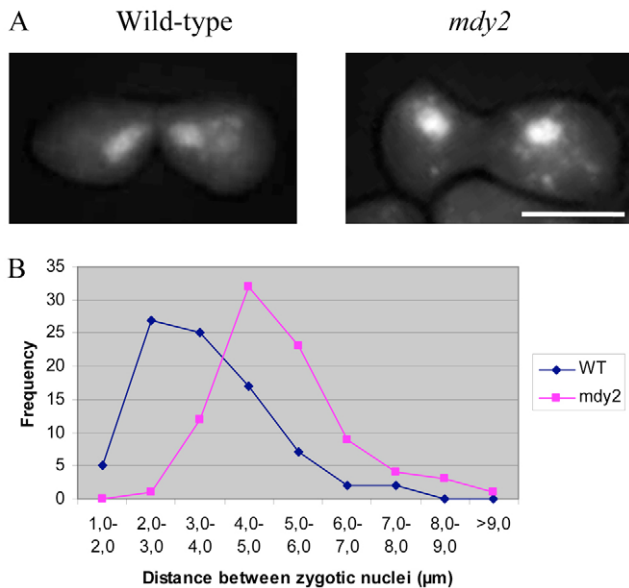

Fig. 4. Distribution of nuclei in wild-type and *mdy2* mutant zygotes 5.5 hours after initiation of mating. The mating mixtures were incubated for 5.5 hours on YPD plates, and the cells were stained with DAPI. Fields of cells containing zygotes were photographed at random for analysis, and the positions of the nuclei were determined. We categorized zygotes according to nuclear positions into one of three classes: pre-nuclear fusion zygotes (class I, top), post-nuclear fusion zygotes (class II, centre), and 'zygotes' in which the haploid nuclei had undergone mitotic division (class III, bottom). 100 zygotes were counted for each cell type.

Fig. 3. Distribution of nuclei in zygotes 3.5 hours after initiation of mating. Cultures of wild-type (HZH638 and HZH639) and *mdy2* mutant (HZH686 and HZH683) strains were grown to log phase. *MAT***a** and *MAT*α cells were mixed and incubated on YPD plates for 3.5 hours to allow zygotes to form. Cells were fixed, stained with DAPI (A), and the distance between the nuclei was measured using the centre of each nucleus as reference (*n*=85 unbudded zygotes for each strain). Bar, 5 μm.
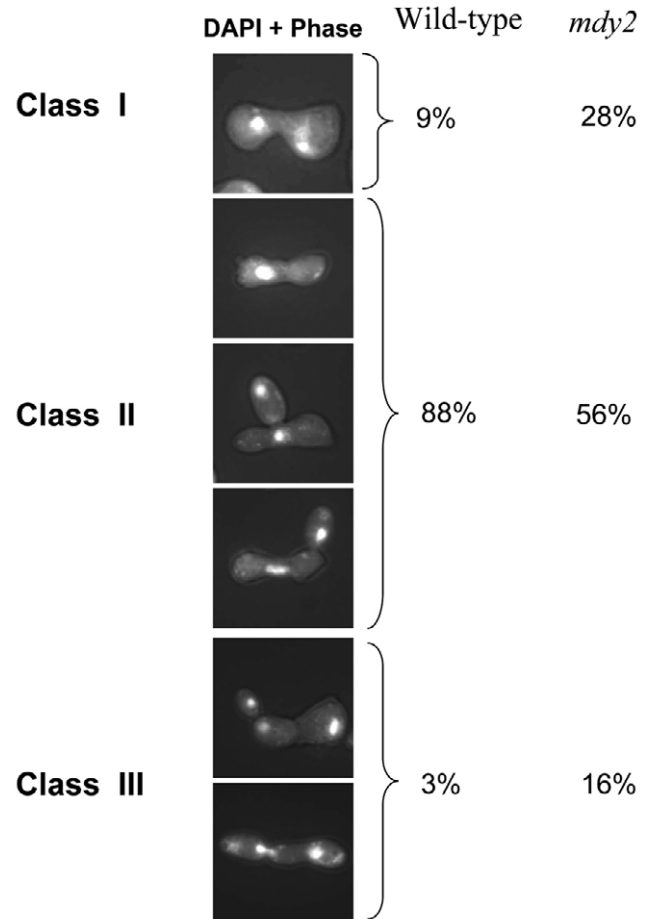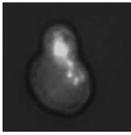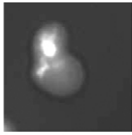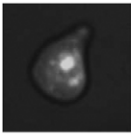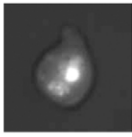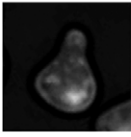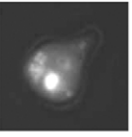
Table 1. Quantitative mating experiments for cytoductants

	X wild-type *MAT*α ρ[+] *CAN*[S]	
	Diploids (%)*	C:D ratio[†]
Wild-type *MAT***a** ρ[0] *can*[R]	31	0.0053
*mdy2 MAT***a** ρ[0] *can*[R]	6	0.13

	X wild-type *MAT***a** ρ[+] *CAN*[S]	
	Diploids (%)*	C:D ratio[†]
Wild-type *MAT*α ρ[0] *can*[R]	33	0.0065
*mdy2 MAT*α ρ[0] *can*[R]	8	0.11

*Percentage diploid formation, which is the number of diploids measured on the selection plates divided by the sum of diploids plus haploid colonies multiplied by 100. [†]Cytoductant:diploid ratio is the number of cytoductants measured on YEP glycerol canavanine plates divided by the number of diploids formed. Strains: wild-type (W303-1A × BY4741) and (W303-1B × BY4742); *mdy2* (HZH686 × BY4741) and (HZH683 × BY4742).

A

The nuclei position in shmoos	Wild-type		*mdy2*	
	DAPI + Phase	Percentage (%)	DAPI + Phase	Percentage (%)
Neck		40		20
Center		56		66
Bottom		4		14

B
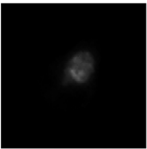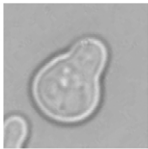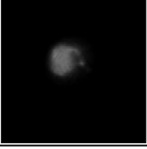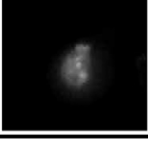
Positions			WT (%)	*mdy2* (%)
	GFP-Nup116	DIC		
Neck			75	40
Middle			22	51
Bottom			3	9

Fig. 5. Determination of nuclear position in wild-type and mutant shmoos. The positions of nuclei in shmoos were classified into three groups: (i) in/at the shmoo neck (top), (ii) in the centre of the cell (centre) or (iii) opposite the mating projection (bottom). The percentage of cells in each class was calculated. *n*>250 shmoos for each strain. (A) Wild-type (HZH638) and *mdy2* mutant strains (HZH686) were induced to form shmoos by treatment with α-factor (5 μM) for 2.5 hours. Cells were fixed, stained with DAPI, and then scored for nuclear position. (B) Cultures of wild-type (W303-1A) and *mdy2* mutant (HZH686) strains harbouring pGAL-*GFP-NUP116* plasmids were grown to log phase and induced in 3% raffinose and 1% galactose medium for 2 hours, and then 5 μM α-factor was added for another 3 hours. After brief fixation, wild-type (WT; W303-1A) and *mdy2* cells were scored for GFP-Nup116 localization (*n*>300).

an increase (36%) in the number of cells with misoriented microtubules (Fig. 6A).

In cells expressing a GFP-Kar9 fusion, the fluorescent signal localizes most frequently to a single spot at the tip of the growing bud and the mating projection (Miller et al., 1999). As expected, in the wild-type shmoos, GFP-Kar9 was localized most frequently (67%) as a dot at the shmoo tip; in a fraction of the cells (22%) the signal formed a line emanating from the shmoo tip (Lee et al., 2000; Matheos et al., 2004; Miller et al., 1999). By contrast, in the *mdy2* mutant 70% of shmoos exhibiting mislocalized GFP-Kar9 (Fig. 6B). From these results, we concluded that the defect in nuclear migration of *mdy2* mutants could be due to a lesion in the process leading to localization of Kar9.

Introduction of *MDY2* into *mdy2* mutants restores the wild-type phenotype

In order to confirm that lack of the MDY2 function is responsible for the mutant phenotypes observed, *mdy2* mutants of both mating types were transformed with 2 μ *MDY2* plasmids. Wild-type cells transformed with the empty 2 μ vector served as controls. The *MAT***a** *mdy2* mutant bearing 2 μ *MDY2* plasmids was crossed to the *MAT*α *mdy2* mutant bearing 2 μ *MDY2* plasmids; this cross resulted in diploid formation with an efficiency of 23±3.7%. The *MAT***a** *MDY2* × *MAT*α *MDY2* cross had an efficiency of 16±2.7%. Thus the overexpression of *MDY2* in the *mdy2* deletants suppressed the mutant phenotype and indeed slightly enhanced mating efficiency relative to the wild-type strain (Fig. 7A). *mdy2*
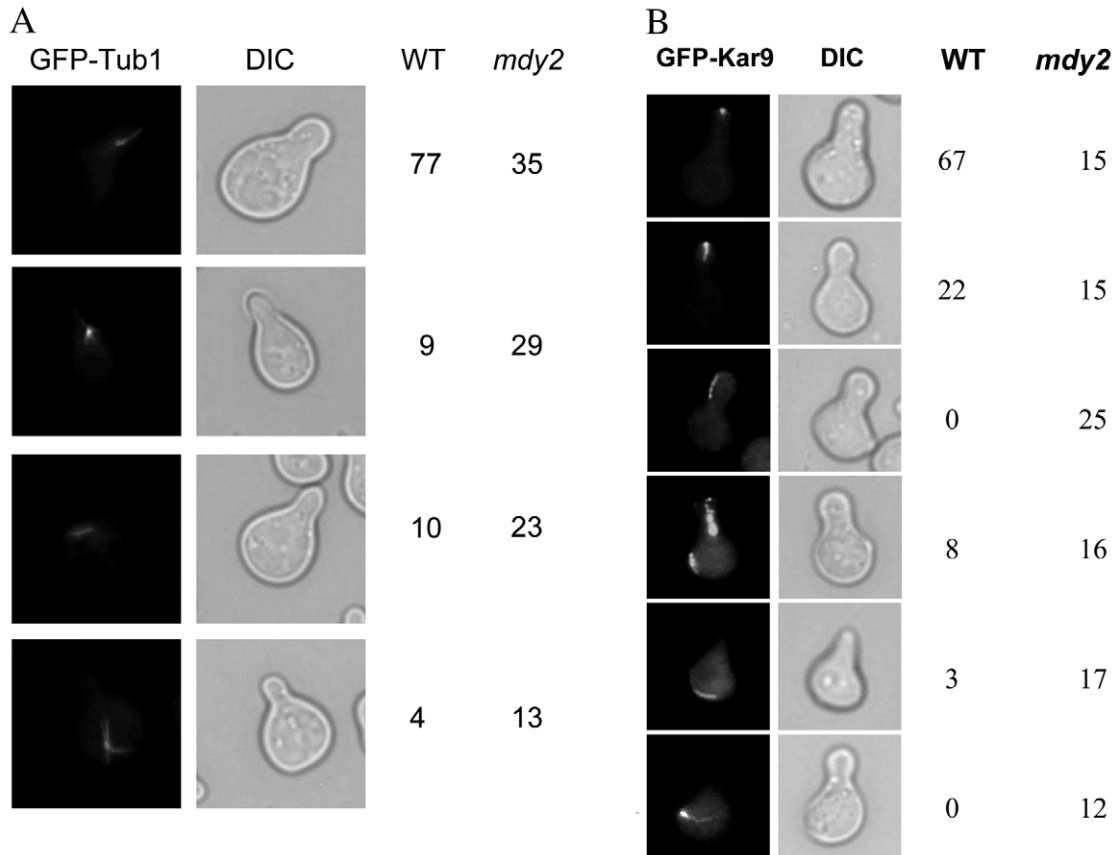
Fig. 6. The *mdy2* mutant shows defects in microtubule orientation and mislocalizes Kar9 in response to pheromone. (A) Cells containing pMET-GFP-TUB1 (pGX388) plasmids were grown to log phase and induced in methionine-free medium for 2 hours; then 5 μM α-factor was added for another 3 hours. After brief fixation, wild-type (WT; HZH638) and *mdy2* (HZH386) cells were scored for GFP-Tub1 localization (*n*>100). Cells were scored as having (from top to bottom): a single bundle of cytoplasmic tubules directed to the shmoo tip, a single bundle of cytoplasmic microtubules going to the shmoo tip plus other bundles oriented away from the shmoo tip, no cytoplasmic microtubules going to the shmoo tip and a spray of microtubules localized on the opposite side to the shmoo. (B) Cells containing p*GAL-GFP-KAR9* were grown in 3% raffinose and 1% galactose for 2 hours, and then pheromone was added for another 3 hours. After brief fixation, wild-type (WT; W303-1A), *mdy2* cells were scored for GFP-Kar9 localization (*n*>250). Cells were scored as having (from top to bottom): a single cortical dot, a line of localization, multiple dots forming a cap near the shmoo tip, or dispersed dots elsewhere in the cell body, possibly on misoriented microtubules.

mutants harbouring 2 μ *MDY2* formed haloes of nearly the same size as the wild-type strain after 48 hours of incubation at 30°C (Fig. 7B). Hence the introduction of 2 μ *MDY2* plasmids into *MATα mdy2* cells also complements the defect in α-factor production observed in *mdy2* deletants.

In order to investigate how overexpression of *MDY2* affects the shmoo index, *MAT**a** mdy2* cells were transformed with 2 μ *MDY2* plasmids or the 2 μ vector. The cells were then treated with 5 μM α-factor, samples were taken at different times, and the numbers of shmoos were counted. The results showed that overexpression of *MDY2* leads to a slight increase in the rate of formation of shmoos as compared with the wild-type strain (Fig. 7C).

GFP-Mdy2 localizes to the nucleus

To study the subcellular localization of Mdy2, we constructed a plasmid carrying *MDY2* fused to the gene for GFP. The GFP-Mdy2 fusion protein was functional in mating assays and complemented the mating defect of the *mdy2* mutant. In vegetatively growing cells, GFP-Mdy2 is localized in the nucleus (Fig. 8A). In cells treated with α-factor, GFP-Mdy2 was also found to be predominantly nuclear (Fig. 8B). Since overexpression may influence the cellular localization of a protein of interest, GFP-*MDY2* was also expressed under the control of the *MDY2* promoter. No change was noted in the localization of the protein (Fig. 8C). Furthermore, after treatment with α-factor, GFP-Mdy2 was still found to be nuclear (Fig. 8D).

Stability of Mdy2 during exposure of cells to pheromone

To study the possible influence of pheromone on the level of Mdy2, a plasmid encoding a GST-tagged version of Mdy2 under the control of the *GAL1* promoter was constructed. A yeast strain bearing this allele was grown to early log phase in SRG medium (3% raffinose and 1% galactose), which permits transcription of GST-*MDY2*. The cells were then transferred to a medium containing glucose (which blocks further transcription of GST-*MDY2*) and 5 μM α-factor (final concentration). Whole cell extracts were prepared from aliquots of the culture at the indicated time points after the
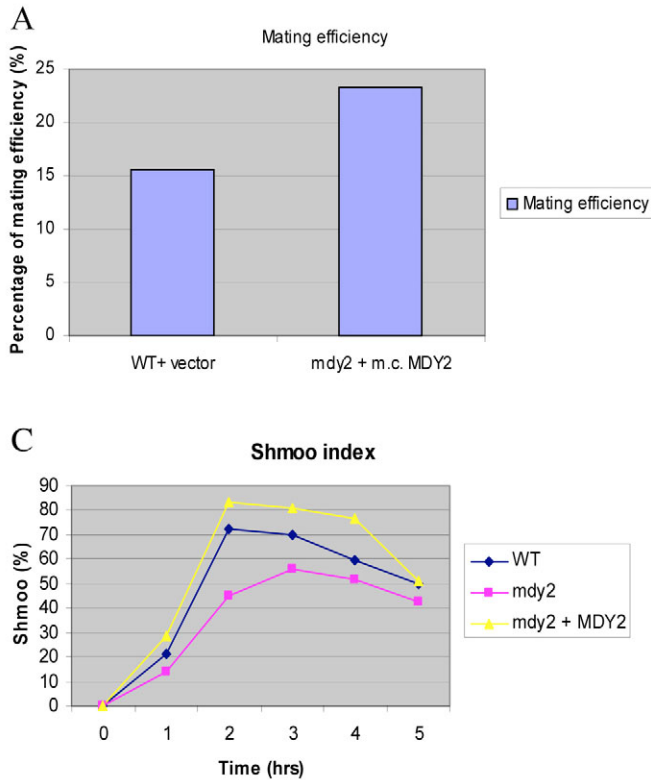
A

B

C

Fig. 7. Analysis of *MDY2* overexpression. (A) Effect of *MDY2* overexpression on mating efficiency. Wild-type strain (W303-1A) was transformed with an empty 2 μ vector (pRS426), *mdy2* mutant (HZH686) were transformed with 2 μ *MDY2* plasmids (pRS426-*MDY2*). The quantitative mating assay was conducted as described in Materials and Methods. The percentage of diploid cells formed is shown. The data are the means of two independent assays. (B) Halo assay for effect of *MDY2* overexpression on α-factor production. 1. *MATα mdy2* mutant cells (HZH683) with an empty 2 μ vector (pRS426). 2. *MATα* wild-type cells (W303-1B) with 2 μ *MDY2* plasmids (pRS426-*MDY2*). 3. *MAT***a** Wild-type cells (W303-1A). 4. *MATα mdy2* mutant cells (HZH683) with 2 μ *MDY2* plasmids (pRS426-*MDY2*). (C) Shmoo index. Wild-type strain W303-1A was transformed with the empty 2 μ vector (pRS426) and the *mdy2* mutant (HZH686) was transformed with the 2 μ *MDY2* plasmid (pRS426-*MDY2*) or pRS426. The cultures were grown in SD medium to log phase and then treated with 5 μM α-factor. Samples were taken at the indicated times and the numbers of shmoos in samples of at least 300 cells were counted.

shift, and GST-*MDY2* was detected by immunoblot analysis with anti-GST antibodies. After galactose depletion and pheromone induction for 90 minutes there is no significant difference in the level of GST-Mdy2, but after 150 minutes a decrease is observed (supplementary material Fig. S2). These data indicate that Mdy2 is relatively stable in the presence of pheromone.

Mdy2 is not subject to C-terminal cleavage

Ubiquitin and UBL proteins, such as NEDD8 or SUMO, are proteolytically processed such that an internal conserved Gly is exposed at the C terminus; this residue is used for their covalent attachment to other proteins. The *MDY2* open reading frame (residues 74-149) exhibits some similarity to ubiquitin and 33% similarity to GdX (Fig. 9A), but lacks glycines proximal to its predicted C terminus. It is, however, conceivable that one of the other conserved residues located near the C terminus is used for processing and conjugation. If Mdy2 acts as a modifier protein, it should be processed to remove non-conserved residue(s) at the C-terminal end. To examine whether processing of Mdy2 occurs, plasmids encoding Myc-Mdy2-H6, GST-Mdy2-H6 and GFP-Mdy2-H6 were constructed. The His-tagged fusion proteins were functional in mating assays and complemented the mating defect of the *mdy2* mutant. Western analysis revealed that extracts of *mdy2Δ* cells expressing Mdy2-His6 from a plasmid retain the C-terminal 6xHis tag, which is detectable with an anti-His antibody in both unstimulated cells and cells treated with α factor (Fig. 9B, left panel). In strains carrying vectors encoding Myc, GST and GFP alone, no band was detected at this level (Fig. 9B and data not shown). It is noteworthy that all three antibodies detect two forms of each fusion protein

(Fig. 9B and data not shown). Mdy2H6 has a molecular mass of 24.5 kDa, but the anti-His antibody labels bands of 24-26 kDa, which may result from non specific partial processing of protease cleavage sites in the spacer region between the N-terminal tags and the Mdy2H6 protein. The intracellular localisation of the Mdy2-His6 variant was determined by immunofluorescence experiments using anti-His antibody (Fig. 9C). Like GFP-Mdy2, the C-terminally His-tagged protein is localized in the nucleus. This result indicates that the tag is not removed by C-terminal processing.

Discussion

The function of the *MDY2* gene was characterized in detail because the corresponding loss-of-function mutant shows a strong impairment in mating and the gene product contains an ubiquitin-like domain (the UBL domain). In quantitative mating assays *mdy2* mutants showed an approximately five to sevenfold reduction in the efficiency of diploid formation. While *mdy2* cells display slight defects in the pheromone signal transduction pathway (data not shown), they have much more severe defects in the formation of shmoos, mating pairs and zygotes. Deletion of *MDY2* causes a 30% reduction in both shmoo and mating pair formation. The strongest effects are seen at the level of zygote formation and mating frequency. The deletion phenotype first becomes manifest during shmoo formation. We find that in *mdy2* cells migration of the nucleus toward the shmoo is delayed or fails to occur. Since shmoo formation itself appears not to be dependent on nuclear migration or attachment (Maddox et al., 2003), Mdy2 might participate in both processes.

Mdy2 is not inducible by pheromone, and is therefore likely to be involved in other processes besides mating. Exposure of

cells to pheromone for 90 minutes did not detectably alter levels of GFP-Mdy2, and only a slight decrease was noted after 150 minutes. We tested several proteins from the pheromone response pathway (Ste50, Ste11, Ste5, Ste7, Fus3, and Kss1) for interaction with Mdy2 but none were detected.

Overexpression of *MDY2* complemented the defects of the *mdy2* mutant such as reduced shmoo formation and α-factor production. The *mdy2* deletion mutant harbouring *MDY2* on a high-copy-number plasmid also showed a slightly higher efficiency of diploid formation than the wild-type strain bearing the empty vector.

In addition, overexpression of *MDY2* under the control of the *GAL1* promoter in *MAT***a** cells led to an increase in the level of induction of *FUS1* in the presence of pheromone (supplementary material Fig. S2), suggesting that Mdy2 can act upon the transcriptional response to mating pheromone.

The *S. cerevisiae* shmoo tip is a model system for analysing the mechanism that couples force production to microtubule plus

ends. The SPB is a trilaminar structure containing a central plaque which is physically embedded in the nuclear envelope, and inner and outer plaques that nucleate the nuclear and cytoplasmic microtubules, respectively (Byers and Goetsch, 1974; Byers and Goetsch, 1975). Dynamic plus ends of astral microtubules, emanating from the SPB, interact with the shmoo tip in mating yeast cells, positioning the nuclei for karyogamy (Maddox et al., 1999). The movement of the nucleus toward the preshmoo and into the shmoo tip occurs via microtubule polymerisation/depolymerisation at the plus end. Individual microtubules grow and shorten in a random search-and-capture process like that described for vegetative G1 cells (Shaw et al., 1997). Once astral microtubules encounter the shmoo tip, subsequent microtubule dynamics results in pushing and/or pulling forces that tether the SPB and nucleus to the shmoo tip (Maddox et al., 1999). Several genes are required for correct positioning of the nuclei. Thus mutants deficient for *KAR3* and *KAR9* are defective in nuclear migration during pheromone induction. Kar9, a putative cortical protein, is required for cytoplasmic microtubule orientation and is thought to anchor the protein Bim1, which attaches to growing microtubule plus ends at the shmoo tip (Miller et al., 2000; Miller and Rose, 1998). Deletion of *KAR3* prevents the attachment of astral microtubules to the shmoo tip, and Kar3 has therefore been proposed to maintain the attachment of depolarising microtubules (Maddox et al., 2003). The fact that nuclear migration toward the developing shmoo in mating cells, and nuclear congression and karyogamy in zygotes, are impaired in *mdy2* cells strongly implies that Mdy2 is involved in the process of nuclear migration. Since mitosis itself is not affected in *mdy2* cells, Mdy2 function seems to be restricted to mating cells, a feature it shares with Kar3. However, unlike Kar3, Mdy2 is mainly localized in the nucleus. Only upon overexpression is a small fraction of the GFP-Mdy2 fusion protein seen in the mating projections. During the pheromone response, *mdy2* mutants were defective in Kar9
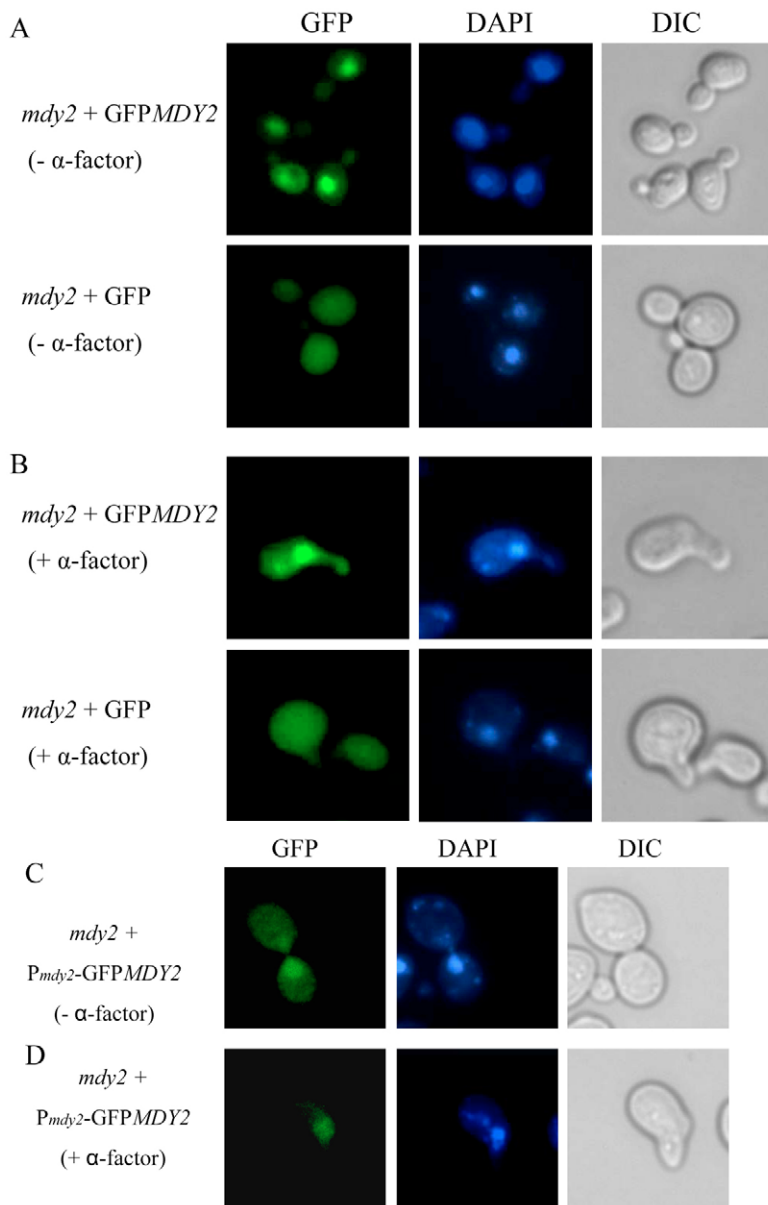

Fig. 8. Localization of Mdy2. (A) Vegetatively growing cells. The mutant *mdy2* (HZH686) was transformed with a plasmid encoding a functional GFP-Mdy2 fusion protein or with the empty vector as a control. Expression of the fusion gene was induced by incubating the cells in 3% raffinose and 1% galactose, and analysed by fluorescence and phase-contrast microscopy. (B) Induction with pheromone. *mdy2* mutant cells were transformed with plasmids expressing a functional GFP-Mdy2 fusion protein or with the empty vector as a control. Cells were induced as above, then treated with 5 μM α-factor for 2 hours, and analysed by fluorescence and phase-contrast microscopy. (C) Expression of GFP-MDY2 under its own promoter. Localization of GFP-Mdy2 expressed under the control of its own promoter. Cultures of the *mdy2* mutant (HZH686) harbouring *MDY2*p-GFP-*MDY2* (pZH152) were grown to log phase. Half of the culture was then harvested and the localization of GFP-Mdy2 fusion protein was investigated. (D) The other half was treated with 5 μM α-factor for 2 hours before fusion protein localization was investigated.
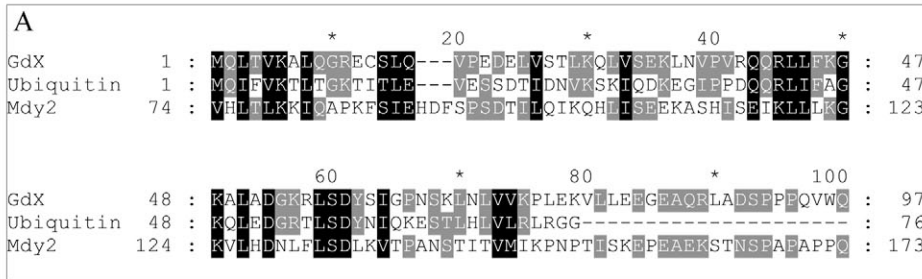
Fig. 9. The Mdy2-6His fusion shows no C-terminal cleavage. (A) Alignment of predicted Mdy2 sequences from residues 74-173 with *S. cerevisiae* ubiquitin and human GdX. Identical residues are shaded in dark grey; similar residues are shaded in light grey. (B) Expression of *MDY2* constructs with C-terminal 6xHis tag is independent of α-factor. Supersensitive *sst2-1* (HGX132) cells carrying the functional GST-Mdy2-H6 construct (N-terminal GST tag and a C-terminal His6 tag) were assayed with 1 μM α-factor and compared with identical untreated cells and cells carrying the GST vector as a negative control. The expression levels were measured by anti-6xHis immunoblot analysis. To control for correct expression, the blot was stripped and reprobed with anti-GST antibody. No anti-His signal could be detected in the GST-negative control (lane 1) and cells not expressing GST at all (lane 4). (C) Localization of Mdy2H6 by indirect immunofluorescence. *mdy2* mutant (HZH686) cells, containing functional GST-Mdy2H6 on a CEN plasmid were prepared as described in Materials and Methods and stained with anti-His antibody (Qiagen) and affinity-purified goat-anti-mouse conjugated to fluorescein (Jackson ImmunoResearch). Micrographs show FITC fluorescence (α-His), DAPI fluorescence and a differential interference contrast (DIC) image. Cells were photographed with Zeiss AxioCam and AxioVision.

localization, and in microtubule alignment. The defect in Kar9 localization and microtubule orientation may indicate that Mdy2 interacts with other proteins that affect the cortical capture of microtubules and spindle orientation. Therefore, Mdy2 may directly or indirectly participates in events at the SPB or other nuclear sites during the migration process; however, a function at the shmoo tip cannot be excluded.

The functional analysis of Mdy2 in this study clearly shows that it is required for efficient mating in *S. cerevisiae* and, unlike most UBL proteins, it is apparently not subject to C-terminal processing. We could not detect any conjugation product of Mdy2 and therefore speculate that it may function by interacting with the UBA domain of a putative target protein. The closest homologue of Mdy2 is the human ubiquitin-like protein GdX, which consists of 157 amino acids.

The shared regions of homology show 34% identity and encompass residues 74-212 of Mdy2 and the N-terminal 123 residues of GdX. Thus the homology extends outside the UBL region (76 amino acids), which shares approx. 20% identity and 20% similarity with ubiquitin (Fig. 9A). *GdX* is a single-copy gene that is conserved in evolution and is regarded as a 'housekeeping' gene that encodes a protein similar to ubiquitin (Toniolo et al., 1988). A growing family of ubiquitin-like proteins has been uncovered in yeast, including Rub1, Dsk2, Rad23, Apg12, Smt3 and Hub1 (Dittmar et al., 2002; Hochstrasser, 1996; Hochstrasser, 2000). The functional consequences of modification by ubiquitin-like proteins appear to be distinct from those associated with ubiquitinylation, in that the ubiquitin-like species do not typically induce the degradation of their protein targets.

Currently, ubiquitin-like proteins are divided into two subclasses (Jentsch and Pyrowolakis, 2000). Type-1 ubiquitin-like polypeptides (UBLs) consist essentially of only the UBL domain and function as modifiers like ubiquitin, being ligated to target proteins in a process similar, but not identical, to the ubiquitylation pathway; they include SUMO, NEDD8 and UCRP/ISG15. In type-2 UBLs (also referred to as UDPs, ubiquitin-domain proteins) the UBL domain is found as part of a larger protein, which obviously has other functions. Among type-2 UBLs are Rad23, Dsk2, Elongin B and GdX, which do not form conjugates with other proteins (Jentsch and Pyrowolakis, 2000). One subclass of UDPs, including Rad23 and Dsk2, contains a UBL domain at the N-terminal end and an ubiquitin association (UBA) domain at the C terminus (Hofmann and Bucher, 1996). Such proteins appear to function as adapter proteins, interacting with both polyubiquitinylated proteins and the 26S proteasome (Chen and Madura, 2002; Elsasser et al., 2004; Funakoshi et al., 2002; Verma et al., 2004). However, the UBA domain may stabilize the protein by interacting with the internal UBL domain (Ortolan et al., 2004). *DSK2* was isolated as a suppressor of *kar1*, which is defective in spindle pole duplication (Biggins et al., 1996). Dsk2 can interact with the proteasome, and an adaptor function in the ubiquitin-proteasome pathway has been discussed (Funakoshi et al., 2002). Our results indicate that Mdy2 is not subject to C-terminal processing or conjugation to other proteins. Mdy2 does not contain a UBA domain, but could interact with UBA domains of other UDPs such as Dsk2. However, Mdy2 was not detected in a two-hybrid screen using an N-terminally truncated Dsk2 (Funakoshi et al., 2002).

In summary, we have found that Mdy2 plays a role in shmoo formation and nuclear congression during the mating process in *S. cerevisiae*. Additional work will be required to unravel its function and the significance of its ubiquitin-like domain.

Materials and Methods

Yeast strains and standard methods
Recombinant DNA techniques were performed according to standard protocols (Sambrook and Russell, 2001). Yeast cells were grown either in YPD medium (2% glucose, 2% peptone, 1% yeast extract) or in synthetic complete (SC) medium (0.67% yeast nitrogen base and 2% glucose), each containing the required nutrient supplements. The strains and plasmids used are listed in Table 2. The *mdy2* mutants were constructed by replacing the entire *MDY2* open reading frame with the *KanMX4* marker. To construct pZH149 (pRS426-*MDY2*), the *MDY2* gene (990 bp) was inserted into the *Spe*I and *Kpn*I sites of the vector pRS426. Plasmid pZH80 (pGREG576GFP-*MDY2*) was constructed by in vivo homologous recombination between the *MDY2* ORF (obtained by PCR) and the vector pGREG576 (Jansen et al., 2005). Plasmid pZH81 (pGREG546GST-*MDY2*) was constructed by in vivo homologous recombination between the *MDY2* ORF and pGREG546. To construct pZH152, the *MDY2* promoter in pGREG576GFP-*MDY2* was replaced by the *GAL1* promoter. The plasmids p526MDY2H6 (Myc-Mdy2-H6), p546MDY2-H6 (GST-Mdy2-H6) and p576MDY2H6 (GFP-Mdy2-H6) were constructed by in vivo recombination between the 0.7-kb MDY2-6xHis fragment and the pGREG vectors (Jansen et al., 2005). PCR fragments were obtained using pYCG-YOL111c (Cognate Gene, EUROSCARF) as template together with the primers 5′-GAATT-CGATATCAAGCTTATCGATACCGTCGACAATGAGCACATCCGCCAGCGG-3′ and 5′-CATGACTCGAGGTCGACTTAGTGATGGTGATGGTGATGTTTGGCC-AGAGACCAGCC-3′.

Quantitative mating assay
Quantitative mating assays were performed as described previously (Elion et al., 1990; Rad et al., 1992). Cultures of opposite mating type (*MAT***a** and *MAT*α) were grown to log phase in SD medium. Equal numbers (3×10^6) of cells of each mating type were mixed and pelleted by centrifugation at 20°C and 10,200 *g* for 4 minutes. The cell pellets were then transferred onto nitrocellulose membranes (NC) placed on YPD plates. The plates were incubated at 30°C for 4.5 hours, after which the cells were transferred to Eppendorf tubes for serial 10-fold dilution. Aliquots (100 μl) of each dilution were spread on SD plates and the plates were incubated at 30°C for 2 days. The total numbers of cells (N_t) and the numbers of diploid cells (N_d) were then counted. The mating efficiency is calculated as the number of colonies of a/α diploids (N_d) divided by the sum of a/α diploids plus haploid colonies (N_t). Crosses between two wild-type strains were used as controls. All tests were carried out in duplicate.

Determination of the shmoo index
Projection formation and budding were assayed essentially as described previously (Xu et al., 1996). Cultures of mutant (*MAT***a** *mut*) and wild-type (*MAT***a**) strains were grown to log phase (OD_{600} 0.2-0.4). α-Factor was added to a final concentration of 5 μM. Samples were taken after incubation with α-factor for 0, 30, 60, 90, 120, 180, 240 and 300 minutes and fixed immediately with 3.7% formaldehyde. Cells were washed twice with 1× PBS buffer prior to microscopy. At least 300 cells per sample were counted and the numbers of shmoos and unbudded cells were recorded. The shmoo index is defined as the percentage of shmoos relative to the total number of cells.

Assay for cell and nuclear fusion
The assay for zygote formation was performed essentially as described previously (Elion et al., 1990; Rad et al., 1992). Cultures of opposite mating type (*MAT***a** and *MAT*α) were grown to log phase in YPD medium. Equal numbers (3×10^6) of cells of each mating type were mixed and pelleted by centrifugation at 20°C and 10,200 *g* for 4 minutes. The cell pellets were transferred onto NC filters on YPD plates, and

Table 2. Yeast strains and plasmids used in this study

Yeast strains	Genotype	Source/Reference
W303-1A	*MAT***a** *leu2-3,112 ura3-1 trp1 his3-11 ade2 can1-100*	R. Rothstein, Columbia University, New York
W303-1B	*MAT*α *leu2-3,112 ura3-1 trp1 his3-11 ade2 can1-100*	R. Rothstein, Columbia University, New York
HZH686	W303-1A *MAT***a** *leu2-3,112 ura3-1 trp1 his3-11 ade2 can1-100Δmdy2::KanMX4*	This work
HZH683	W303-1B *MAT*α *leu2-3,112 ura3-1 trp1 his3-11 ade2 can1-100Δmdy2::KanMX4*	This work
HGX132	MG5D *MAT***a** *sst2-1 ura3-1 his3-11,1, his4-580 leu2 lys2 tyr1 trp1*	M.R.-R.'s laboratory
HGX133	MG6B *MAT*α *sst2-1 ura3-1 his3-11,15 ade2 trp1*	M.R.-R.'s laboratory
BY4741	*MAT***a** *ura3 his3-1 leu2 met15*	(Brachmann et al., 1998)
BY4742	*MAT*α *ura3 his3-1 leu2 lys2*	(Brachmann et al., 1998)
HZH350	BY4741 *MAT***a** *Δsst1 (bar1) ura3 his3-1 leu2 met15* (BY01408)	Euroscarf (Brachmann et al., 1998)

Plasmids	Description	Source/Reference
pRS426	pBluescript; *URA3;* 2μ	(Christianson et al., 1992)
pSB234	*FUS1*-promoter-*lacZ; URA3;* 2μ	(Trueheart and Fink, 1989)
pUG6	P*FAG-KanMX4, TEF2* promoter, *TEF2* terminator; *URA3;* CEN	(Guldener et al., 1996)
pGREG576	*GAL*1-promotor-GFP; *CYC1* terminator; *URA3;* CEN	(Jansen et al., 2005)
pZH80	pGREG576-*MDY2*; *URA3;* CEN	This work
pZH81	pGREG546GST-*MDY2*; *URA3;* CEN	This work
pZH152	pRS416-*MDY2*p-GFP-*MDY2*; *URA3;* CEN	This work
pZH192	pGREG576-*NUP116*; *URA3;* CEN	This work
pGX388	pRS424-*MET25*-GFP-*TUB1; TRP1;* 2μ	M.R.-R.'s laboratory
pMR3465	p*GAL1-GFP-KAR9; LEU2; CEN*	(Matheos et al., 2004)

incubated at 30°C for various times (1, 2, 3, 4 and 5 hours). The cells on each membrane were then washed off with 1 ml of sterile water, and pelleted by centrifugation at 20°C and 10,200 *g* for 4 minutes. The pellets were resuspended in 1× PBS buffer and fixed with 70% ethanol. Cells were washed twice with 1× PBS buffer prior to observation under the microscope. The proportions of zygotes were counted in samples containing at least 800 cells, and the efficiency of zygote formation was calculated. Nuclei were stained with DAPI (4′,6-diamidino-Z-phenylindole; 1 μg/ml), and the different stages of zygote development were analyzed under the microscope. The numbers of pre-zygotes (with unfused nuclei), zygotes and abnormal zygotes in samples containing at least 200 zygotes were determined. Cytoductant analysis and microscopic analysis of the zygotes (Berlin et al., 1991; Gammie and Rose, 2002) were performed to detect defects in cell and nuclear fusion. ρ^0 strains were obtained by growing cultures in aluminium foil-wrapped flasks containing YPD and 10 μg/ml ethidium bromide at 30°C overnight. The cultures were spread on YPD plates and incubated at 30°C. After a 2-day incubation the colonies were replicated onto YEP glycerol plates and incubated at 30°C. ρ^0 strains (completely lacking mitochondrial DNA) were identified by DAPI staining. ρ^0 (can^R) and ρ^+ (CAN^S) strains were grown to log phase and approximately equal numbers of cells (3×10^6) were mixed and mated for 4 hours on an NC filter (0.45 μm pore size). Samples were collected and 10-fold serial dilutions (10^{-1}, 10^{-2}, 10^{-3} and 10^{-4}) were prepared using sterile water. Samples (100 μl) were plated onto synthetic complete medium minus arginine containing 3% glycerol and canavanine (60 μg/ml). The total numbers of cells and diploids were determined by plating dilutions of the mating mixture onto minimal media. The efficiency of nuclear fusion is expressed as the ratio of cytoductants to diploids (C:D).

Microscopy

Cultures of strains harbouring a plasmid carrying the *GFP*-tagged genes under the control of the *GAL1* promoter were grown to log phase in SRG medium. Cells were harvested and washed with 1× PBS buffer (pH 7.4) in Eppendorf tubes. The cells were sonicated briefly to break up aggregates, and fixed with 70% ethanol for 12 minutes. Then the cells were washed again with 1× PBS buffer, stained with DAPI at room temperature for 12 minutes, and washed again with 1× PBS buffer. The distribution of tagged fusion protein and nuclei was investigated by fluorescence microscopy. Cells were processed for immunofluorescence essentially as described previously (Pringle et al., 1989). Cells were grown to exponential phase (OD$_{600}$=0.5-0.8, 3-4×10^7/ml) and immediately fixed with formaldehyde (final concentration 5% for 4 hours). The fixed cells were spheroplasted and extracted with 0.1% Triton X-100 for 5 minutes and then attached to a multiwell slide treated with 0.1% poly-lysine (Sigma, St Louis, MO, USA). The cells were first incubated with an anti-His mouse monoclonal antibody (Qiagen; 1:200 dilution in PBS plus 1 mg/ml bovine serum albumin) for 90 minutes and then for 90 minutes with fluorescein isothiocyanate (FITC)-conjugated anti-mouse antibodies (Dianova, Hamburg, Germany; 1:300 dilution in PBS/BSA). Finally, the cells were incubated for 5 minutes with DAPI (1 μg/ml). Fluorescence was visualized with an Axioskop fluorescence microscope (Zeiss, Oberkochen, Germany) using a FITC filter set, and images were obtained with a Zeiss AxioCam digital camera.

Gene disruption

Gene disruption in *S. cerevisiae* was performed according to the method described previously (Gueldener et al., 2002). The fragment carrying the *LoxP-kanMX-LoxP* disruption cassette was amplified by PCR. PCR products were precipitated with ethanol, recovered by centrifugation and dissolved in 10 μl of water. Yeast cells were transformed with the *LoxP-kanMX-LoxP* disruption cassette by the high-efficiency LiAc transformation method. Single colonies were isolated from YPD plates containing G418 and prepared for further analysis. A well separated colony growing on an YPD plate containing G418 was picked with a pipette tip and resuspended in 40 μl of 0.02 M NaOH solution in an Eppendorf tube. The tube was heated in a microwave for 90 seconds, and then incubated at room temperature for 30 minutes. The sample was then stored at –20°C for 1 hour. PCR was subsequently performed to check the length of the fragments.

Galactose depletion assay

The galactose depletion assay was performed according to a previously described protocol (Esch and Errede, 2002). Cultures were first grown to early log phase in the appropriate selective medium containing 3% raffinose and 1% galactose to induce expression of p*GAL-GST-MDY2*. Cells were then harvested, washed, and transferred to medium containing 2% glucose to inhibit further transcription of the fusion gene. After the removal of a control sample, incubation of the cultures was continued with or without (5 μM) α-factor to activate the mating pheromone response pathway. Whole cell extracts were then prepared for immunoblot analysis.

References

Andrews, B. J. and Herskowitz, I. (1990). Regulation of cell cycle-dependent gene expression in yeast. *J. Biol. Chem.* **265**, 14057-14060.

Arkowitz, R. A. (1999). Responding to attraction: chemotaxis and chemotropism in Dictyostelium and yeast. *Trends Cell. Biol.* **9**, 20-27.

Berlin, V., Brill, J. A., Trueheart, J., Boeke, J. D. and Fink, G. R. (1991). Genetic screens and selections for cell and nuclear fusion mutants. *Methods Enzymol.* **194**, 774-792.

Biggins, S., Ivanovska, I. and Rose, M. D. (1996). Yeast ubiquitin-like genes are involved in duplication of the microtubule organizing center. *J. Cell Biol.* **133**, 1331-1346.

Brachmann, C. B., Davies, A., Cost, G. J., Caputo, E., Li, J., Hieter, P. and Boeke, J. D. (1998). Designer deletion strains derived from Saccharomyces cerevisiae S288C: a useful set of strains and plasmids for PCR-mediated gene disruption and other applications. *Yeast* **14**, 115-132.

Burkholder, A. C. and Hartwell, L. H. (1985). The yeast alpha-factor receptor: structural properties deduced from the sequence of the STE2 gene. *Nucleic Acids Res.* **13**, 8463-8475.

Byers, B. and Goetsch, L. (1974). Duplication of spindle plaques and integration of the yeast cell cycle. *Cold Spring Harb. Symp. Quant. Biol.* **38**, 123-131.

Byers, B. and Goetsch, L. (1975). Behavior of spindles and spindle plaques in the cell cycle and conjugation of *Saccharomyces cerevisiae*. *J. Bacteriol.* **124**, 511-523.

Carminati, J. L. and Stearns, T. (1997). Microtubules orient the mitotic spindle in yeast through dynein-dependent interactions with the cell cortex. *J. Cell Biol.* **138**, 629-641.

Chant, J. (1999). Cell polarity in yeast. *Annu. Rev. Cell Dev. Biol.* **15**, 365-391.

Chen, L. and Madura, K. (2002). Rad23 promotes the targeting of proteolytic substrates to the proteasome. *Mol. Cell. Biol.* **22**, 4902-4913.

Chenevert, J., Valtz, N. and Herskowitz, I. (1994). Identification of genes required for normal pheromone-induced cell polarization in Saccharomyces cerevisiae. *Genetics* **136**, 1287-1296.

Christianson, T. W., Sikorski, R. S., Dante, M., Shero, J. H. and Hieter, P. (1992). Multifunctional yeast high-copy-number shuttle vectors. *Gene* **110**, 119-122.

Cross, F., Hartwell, L. H., Jackson, C. and Konopka, J. B. (1988). Conjugation in *Saccharomyces cerevisiae*. *Annu. Rev. Cell Biol.* **4**, 429-457.

Dittmar, G. A., Wilkinson, C. R., Jedrzejewski, P. T. and Finley, D. (2002). Role of a ubiquitin-like modification in polarized morphogenesis. *Science* **295**, 2442-2446.

Dorer, R., Boone, C., Kimbrough, T., Kim, J. and Hartwell, L. H. (1997). Genetic analysis of default mating behavior in Saccharomyces cerevisiae. *Genetics* **146**, 39-55.

Elion, E. A. (1995). Ste5: a meeting place for MAP kinases and their associates. *Trends Cell Biol.* **5**, 322-327.

Elion, E. A., Grisafi, P. L. and Fink, G. R. (1990). FUS3 encodes a cdc2+/CDC28-related kinase required for the transition from mitosis into conjugation. *Cell* **60**, 649-664.

Elsasser, S., Chandler-Militello, D., Muller, B., Hanna, J. and Finley, D. (2004). Rad23 and Rpn10 serve as alternative ubiquitin receptors for the proteasome. *J. Biol. Chem.* **279**, 26817-26822.

Esch, R. K. and Errede, B. (2002). Pheromone induction promotes Ste11 degradation through a MAPK feedback and ubiquitin-dependent mechanism. *Proc. Natl. Acad. Sci. USA* **99**, 9160-9165.

Fabre, E. and Hurt, E. (1997). Yeast genetics to dissect the nuclear pore complex and nucleocytoplasmic trafficking. *Annu. Rev. Genet.* **31**, 277-313.

Funakoshi, M., Sasaki, T., Nishimoto, T. and Kobayashi, H. (2002). Budding yeast Dsk2p is a polyubiquitin-binding protein that can interact with the proteasome. *Proc. Natl. Acad. Sci. USA* **99**, 745-750.

Gammie, A. E. and Rose, M. D. (2002). Assays of cell and nuclear fusion. *Methods Enzymol.* **351**, 477-498.

Gueldener, U., Heck, S., Fielder, T., Beinhauer, J. and Hegemann, J. H. (1996). A new efficient gene disruption cassette for repeated use in budding yeast. *Nucleic Acids Res.* **24**, 2519-2524.

Gueldener, U., Heinisch, J., Koehler, G. J., Voss, D. and Hegemann, J. H. (2002). A second set of loxP marker cassettes for Cre-mediated multiple gene knockouts in budding yeast. *Nucleic Acids Res.* **30**, e23.

Heiman, M. G. and Walter, P. (2000). Prm1p, a pheromone-regulated multispanning membrane protein, facilitates plasma membrane fusion during yeast mating. *J. Cell Biol.* **151**, 719-730.

Herskowitz, I. (1995). MAP kinase pathways in yeast: for mating and more. *Cell* **80**, 187-197.

Herskowitz, I., Park, H. O., Sanders, S., Valtz, N. and Peter, M. (1995). Programming of cell polarity in budding yeast by endogenous and exogenous signals. *Cold Spring Harb. Symp. Quant. Biol.* **60**, 717-727.

Hochstrasser, M. (1996). Ubiquitin-dependent protein degradation. *Annu. Rev. Genet.* **30**, 405-439.

Hochstrasser, M. (2000). Evolution and function of ubiquitin-like protein-conjugation systems. *Nat. Cell. Biol.* **2**, E153-E157.

Hofmann, K. and Bucher, P. (1996). The UBA domain: a sequence motif present in multiple enzyme classes of the ubiquitination pathway. *Trends Biochem. Sci.* **21**, 172-173.

Iwanejko, L., Smith, K. N., Loeillet, S., Nicolas, A. and Fabre, F. (1999). Disruption and functional analysis of six ORFs on chromosome XV: YOL117w, YOL115w (TRF4), YOL114c, YOL112w (MSB4), YOL111c and YOL072w. *Yeast* **15**, 1529-1539.

Jansen, G., Wu, C., Schade, B., Thomas, D. Y. and Whiteway, M. (2005). Drag&Drop cloning in yeast. *Gene* **344**, 43-51.

Jentsch, S. and Pyrowolakis, G. (2000). Ubiquitin and its kin: how close are the family ties? *Trends Cell Biol.* **10**, 335-342.

Johnson, D. I. and Pringle, J. R. (1990). Molecular characterization of CDC42, a Saccharomyces cerevisiae gene involved in the development of cell polarity. *J. Cell Biol.* **111**, 143-152.

Lee, L., Tirnauer, J. S., Li, J., Schuyler, S. C., Liu, J. Y. and Pellman, D. (2000). Positioning of the mitotic spindle by a cortical-microtubule capture mechanism. *Science* **287**, 2260-2262.

Leeuw, T., Fourest-Lieuvin, A., Wu, C., Chenevert, J., Clark, K., Whiteway, M., Thomas, D. Y. and Leberer, E. (1995). Pheromone response in yeast: association of Bem1p with proteins of the MAP kinase cascade and actin. *Science* **270**, 1210-1213.

Maddox, P., Chin, E., Mallavarapu, A., Yeh, E., Salmon, E. D. and Bloom, K. (1999). Microtubule dynamics from mating through the first zygotic division in the budding yeast Saccharomyces cerevisiae. *J. Cell Biol.* **144**, 977-987.

Maddox, P. S., Stemple, J. K., Satterwhite, L., Salmon, E. D. and Bloom, K. (2003). The minus end-directed motor Kar3 is required for coupling dynamic microtubule plus ends to the cortical shmoo tip in budding yeast. *Curr. Biol.* **13**, 1423-1428.

Matheos, D., Metodiev, M., Muller, E., Stone, D. and Rose, M. D. (2004). Pheromone-induced polarization is dependent on the Fus3p MAPK acting through the formin Bni1p. *J. Cell Biol.* **165**, 99-109.

Miller, R. K. and Rose, M. D. (1998). Kar9p is a novel cortical protein required for cytoplasmic microtubule orientation in yeast. *J. Cell Biol.* **140**, 377-390.

Miller, R. K., Cheng, S. C. and Rose, M. D. (2000). Bim1p/Yeb1p mediates the Kar9p-dependent cortical attachment of cytoplasmic microtubules. *Mol. Biol. Cell* **11**, 2949-2959.

Miller, R. K., Matheos, D. and Rose, M. D. (1999). The cortical localization of the microtubule orientation protein, Kar9p, is dependent upon actin and proteins required for polarization. *J. Cell Biol.* **144**, 963-975.

Nern, A. and Arkowitz, R. A. (2000). G proteins mediate changes in cell shape by stabilizing the axis of polarity. *Mol. Cell* **5**, 853-864.

Ortolan, T. G., Chen, L., Tongaonkar, P. and Madura, K. (2004). Rad23 stabilizes Rad4 from degradation by the Ub/proteasome pathway. *Nucleic Acids Res.* **32**, 6490-6500.

Pringle, J. R., Preston, R. A., Adams, A. E., Stearns, T., Drubin, D. G., Haarer, B. K. and Jones, E. W. (1989). Fluorescence microscopy methods for yeast. *Methods Cell Biol.* **31**, 357-435.

Rad, M. R., Xu, G. and Hollenberg, C. P. (1992). STE50, a novel gene required for activation of conjugation at an early step in mating in Saccharomyces cerevisiae. *Mol. Gen. Genet.* **236**, 145-154.

Read, E. B., Okamura, H. H. and Drubin, D. G. (1992). Actin- and tubulin-dependent functions during Saccharomyces cerevisiae mating projection formation. *Mol. Biol. Cell* **3**, 429-444.

Roemer, T., Madden, K., Chang, J. and Snyder, M. (1996). Selection of axial growth sites in yeast requires Axl2p, a novel plasma membrane glycoprotein. *Genes Dev.* **10**, 777-793.

Rose, M. D. (1991). Nuclear fusion in yeast. *Annu. Rev. Microbiol.* **45**, 539-567.

Rose, M. D. (1996). Nuclear fusion in the yeast Saccharomyces cerevisiae. *Annu. Rev. Cell Dev. Biol.* **12**, 663-695.

Saeki, Y., Saitoh, A., Toh-e, A. and Yokosawa, H. (2002). Ubiquitin-like proteins and Rpn10 play cooperative roles in ubiquitin-dependent proteolysis. *Biochem. Biophys. Res. Commun.* **293**, 986-992.

Sambrook, J. and Russell, D. W. (2001). *Molecular Cloning, A Laboratory Manual.* New York: Cold Spring Harbor Laboratory Press.

Segall, J. E. (1993). Polarization of yeast cells in spatial gradients of alpha mating factor. *Proc. Natl. Acad. Sci. USA* **90**, 8332-8336.

Shaw, S. L., Yeh, E., Maddox, P., Salmon, E. D. and Bloom, K. (1997). Astral microtubule dynamics in yeast: a microtubule-based searching mechanism for spindle orientation and nuclear migration into the bud. *J. Cell Biol.* **139**, 985-994.

Sheu, Y. J., Santos, B., Fortin, N., Costigan, C. and Snyder, M. (1998). Spa2p interacts with cell polarity proteins and signaling components involved in yeast cell morphogenesis. *Mol. Cell. Biol.* **18**, 4053-4069.

Sprague, G., Jr and Thorner, J. (1992). Pheromone response and signal transduction during the mating process of *Saccharomyces cerevisiae*. In *The Molecular Biology of the Yeast Saccharomyces cerevisiae* (ed. J. R. Broach, J. R. Pringle and E. W. Jones), pp. 657-744. New York: Cold Spring Harbor Laboratory Press.

Sprague, G. F., Jr, Jensen, R. and Herskowitz, I. (1983). Control of yeast cell type by the mating type locus: positive regulation of the alpha-specific STE3 gene by the MAT alpha 1 product. *Cell* **32**, 409-415.

Toniolo, D., Martini, G., Migeon, B. R. and Dono, R. (1988). Expression of the G6PD locus on the human X chromosome is associated with demethylation of three CpG islands within 100 kb of DNA. *EMBO J.* **7**, 401-406.

Trueheart, J. and Fink, G. R. (1989). The yeast cell fusion protein FUS1 is O-glycosylated and spans the plasma membrane. *Proc. Natl. Acad. Sci. USA* **86**, 9916-9920.

Verma, R., Oania, R., Graumann, J. and Deshaies, R. J. (2004). Multiubiquitin chain receptors define a layer of substrate selectivity in the ubiquitin-proteasome system. *Cell* **118**, 99-110.

Xu, G., Jansen, G., Thomas, D. Y., Hollenberg, C. P. and Ramezani Rad, M. (1996). Ste50p sustains mating pheromone-induced signal transduction in the yeast Saccharomyces cerevisiae. *Mol. Microbiol.* **20**, 773-783.